

# Magnetic vortex in color-flavor locked quark matter

Kei Iida

*RIKEN BNL Research Center, Brookhaven National Laboratory, Upton, New York 11973*

(Dated: October 25, 2018)

Within Ginzburg-Landau theory, we study the structure of a magnetic vortex in color-flavor locked quark matter. This vortex is characterized by winding of the  $SU(3)$  phase in color-flavor space, as well as by the presence of a color-flavor unlocked condensate in the core. We estimate the upper and lower critical fields and the critical Ginzburg-Landau parameter that distinguishes between type I and type II superconductors.

PACS numbers: 12.38.Mh, 26.60.+c

## I. INTRODUCTION

The possibility that dense quark matter occurs in neutron stars has been considered for the past three decades. The possible presence of a diquark condensate in such quark matter [1] has generated new interest in such matter. Among various condensates, a color-flavor locked (CFL) state [2], in which all three color and flavors are gapped, has been studied most intensively, along with a two-flavor pairing state [3]. In the weak coupling (high density) and massless limit the CFL state is most stable at zero temperature [4] and near the transition temperature [5], a feature ensured by the quark-quark attraction in the color antitriplet channel due to one-gluon exchange. Although the massless, weak coupling results for diquark condensation are modified by effects of strong coupling and nonzero quark masses in a regime as might be encountered in possible quark matter in neutron star interiors [6], the CFL phase has to be reckoned with as a reference state in such a regime.

Response of the CFL condensate to magnetic fields, as would be experienced by quark matter if present in neutron stars, was considered in Refs. [3, 7, 8, 9, 10]. Because of nonvanishing color and electric charge carried by diquark pairs, electromagnetic superconductivity and color superconductivity occur in the CFL phase. These two phenomena are not independent in the sense that transverse photon and gluon fields are mixed with each other. One of the resultant mixed fields is freely propagating, while the other is Meissner screened and thus massive. The massive mixed field and the winding of the  $SU(3)$  phase in color-flavor space are essential to the structure of a magnetic vortex in the CFL phase. This point was not taken into account in Ref. [9]. The criterion of whether or not the CFL state can allow magnetic vortices to form (type II or type I) has been described by Giannakis and Ren [10] in terms of the energy needed to form a planar surface separating the normal and superconducting material, but the detailed structure of the magnetic vortex has yet to be determined.

In this paper we examine the properties of magnetic vortices in the CFL phase within the framework of Ginzburg-Landau theory. These vortices are characterized by three different fields: the CFL diquark field, the massive photon-gluon mixed field, and a color-flavor unlocked diquark field coupled to the mixed field [10]. In the London limit where the wavelengths of distortions of the condensate are long compared with the size of the vortex core, the supercurrents surrounding the core can be written in terms of the color-flavor  $SU(3)$  phase of the CFL condensate and the mixed field. From such supercurrent structures we derive the lower critical field,  $H_{c1}$ . We next examine the vortex structure near the core, in which the color-flavor unlocked condensate plays a role, and derive the upper critical field,  $H_{c2}$ . Finally we revisit how to distinguish between type I and type II superconductors from the viewpoint of the intervortex interactions. Throughout this paper, we consider a system of three-flavor ( $uds$ ) and three-color ( $RGB$ ) massless quarks at temperature  $T$  and baryon chemical potential  $\mu$ , and use units  $\hbar = c = 1$ . We assume that the Fermi momentum is common to all colors and flavors since in the massless limit of interest here, it is the case with both the normal and CFL phases of equilibrated neutral quark matter.

## II. GINZBURG-LANDAU THEORY

We first review the Ginzburg-Landau theory relevant for the description of the CFL phase [5, 9, 10]. While this theory is strictly applicable near the critical temperature  $T_c$  and for inhomogeneities of wavelengths longer than the zero temperature coherence length  $\xi_0 \sim T_c^{-1}$ , it is nevertheless useful in describing the structure of a possible vortex in the presence of external uniform magnetic fields. This theory focuses only on the pairing channel that first prevails in a normal quark-gluon plasma as the temperature goes down. In the weak coupling (high density) regime, this pairing channel is predicted to have even parity, zero total angular momentum, and same chirality, and to be in a color and flavor antitriplet state. As we shall see, the CFL phase belongs to this pairing channel. We assume that this channel

has the highest transition temperature also at lower densities. This pairing state is characterized by a complex  $3 \times 3$  gap matrix,  $(\mathbf{d}_a)_i(\mathbf{r})$ , in color-flavor space [5], where  $a$  ( $i$ ) is the color (flavor) other than two colors (flavors) involved in Cooper pairing. This gap is defined on the mass shell of the quark quasiparticle of momenta on the Fermi surface, but remains dependent on the center-of-mass coordinate  $\mathbf{r}$  of the quark Cooper pair.

In the presence of an external magnetic field,  $\mathbf{H}_{\text{ext}} = \nabla \times \mathbf{A}_{\text{ext}}$ , one can write down the thermodynamic potential density difference  $\Delta\Omega = \Omega_s - \Omega_n$  between the superfluid and normal phases near  $T_c$  as [9]

$$\Delta\Omega = \bar{\alpha} \sum_a |\mathbf{d}_a|^2 + \beta_1 \left( \sum_a |\mathbf{d}_a|^2 \right)^2 + \beta_2 \sum_{ab} |\mathbf{d}_a^* \cdot \mathbf{d}_b|^2 + 2K_T \sum_a |(D_l \mathbf{d})_a|^2 + \frac{1}{4} G_{lm}^\alpha G_{lm}^\alpha + \frac{1}{4} F_{lm} F_{lm} - \frac{1}{2} |\mathbf{H}_{\text{ext}}|^2. \quad (1)$$

Here we have neglected the response of the normal component to  $\mathbf{H}_{\text{ext}}$ . The parameters  $\bar{\alpha}$ ,  $\beta_1$ , and  $\beta_2$  characterize the homogeneous part of the free energy, while  $K_T$  is the stiffness parameter, controlling spatial variations of the order parameter. Since  $(\mathbf{d}_a)_i$  is antisymmetric in color and flavor space, the covariant derivative  $D_l$  is

$$(D_l \mathbf{d})_a = \partial_l \mathbf{d}_a - \frac{i}{2} g A_l^\alpha (\lambda^\alpha \mathbf{d})_a - i e A_l (Q \mathbf{d})_a, \quad (2)$$

where the  $\lambda^\alpha$  are the Gell-Mann matrices.  $G_{lm}^\alpha$  ( $F_{lm}$ ) is the spatial part of the gluon (photon) field-strength tensor,  $Q = \text{diag}(2, -1, -1)/3$  is the electric charge matrix in flavor space, and  $g$  is the QCD coupling constant. Here we have adopted the convention in which  $\lambda^8 = \text{diag}(2, -1, -1)/\sqrt{3}$  and  $(\mathbf{d}_a)_i$  is defined in terms of the adjoint spinors, rather than the spinors [11].

The parameters  $\bar{\alpha}$ ,  $\beta_1$ ,  $\beta_2$ , and  $K_T$  in Eq. (1) can in principle be determined as functions of  $T$  and  $\mu$ . In a general Ginzburg-Landau framework, however, these parameters are left unknown. The parameters have been determined only in the weak coupling limit in which the pairing interaction is controlled by Landau-damped magnetic gluons, and are [5, 12]

$$\bar{\alpha} = 4N(\mu/3) \ln \left( \frac{T}{T_c} \right), \quad (3)$$

$$\beta_1 = \beta_2 = 3K_T = \frac{7\zeta(3)}{8(\pi T_c)^2} N(\mu/3), \quad (4)$$

$$N(\mu/3) = \frac{1}{2\pi^2} \left( \frac{\mu}{3} \right)^2, \quad (5)$$

with the zeta function  $\zeta(3) = 1.202 \dots$ .

In homogeneous quark matter in weak coupling, the energy difference (1) has a minimal value [5] just below  $T_c$  for a CFL order parameter, i.e.,

$$(\mathbf{d}_a)_i = U_{ai} \kappa_A, \quad \kappa_A = e^{i\varphi_0} |\kappa_A|, \quad (6)$$

where  $U \equiv \exp(i\lambda^\alpha \varphi_\alpha/2)$  represents  $SU(3)$  rotations in color-flavor space. Generally, in a homogeneous situation, the CFL state is the most stable as long as  $3\beta_1 + \beta_2 > 0$  and  $\beta_2 > 0$  [5]. In terms of  $\bar{\alpha}$ ,  $\beta_1$ , and  $\beta_2$ , the minimizing value of  $|\kappa_A|$  is

$$|\kappa_A| = \left( \frac{-\bar{\alpha}}{6\beta_{\text{CFL}}} \right)^{1/2}, \quad (7)$$

where  $\bar{\beta}_{\text{CFL}} = \beta_1 + \beta_2/3$ .

We can now derive the field equations characterizing the CFL state under constant external magnetic field,  $\mathbf{H}_{\text{ext}}$ . In this situation, as clarified in Ref. [10], the electromagnetic field, which is mixed with the gluon field of  $\alpha = 8$ , is coupled with the color-flavor rotation  $\exp(i\lambda^8 \varphi_8/2)$  of the gap matrix  $(\mathbf{d}_a)_i$ . Interestingly, the solution to the field equations requires a nonvanishing color-flavor unlocked diquark component proportional to  $[\lambda^8 \exp(i\lambda^8 \varphi_8/2)]_{ai}$ , in addition to the CFL component proportional to  $[\exp(i\lambda^8 \varphi_8/2)]_{ai}$  [10]; addition of any other components would simply increase the total free energy of the system. It is thus convenient to introduce the ansatz for the pairing gap [10]:

$$\begin{aligned} (\mathbf{d}_a)_i(\mathbf{r}) &= \delta_{aR} \delta_{iu} \phi(\mathbf{r}) + (\delta_{aG} \delta_{id} + \delta_{aB} \delta_{is}) \chi(\mathbf{r}) / \sqrt{2} \\ &= [e^{i\lambda^8 \varphi_8(\mathbf{r})/2}]_{ai} \frac{|\phi(\mathbf{r})| + \sqrt{2} |\chi(\mathbf{r})|}{3} + \left[ \frac{\lambda_8}{2} e^{i\lambda^8 \varphi_8(\mathbf{r})/2} \right]_{ai} \frac{2|\phi(\mathbf{r})| - \sqrt{2} |\chi(\mathbf{r})|}{\sqrt{3}}, \end{aligned} \quad (8)$$

with  $\phi(\mathbf{r}) = \exp[i\varphi_8(\mathbf{r})/\sqrt{3}]|\phi(\mathbf{r})|$  and  $\chi(\mathbf{r}) = \exp[-i\varphi_8(\mathbf{r})/2\sqrt{3}]|\chi(\mathbf{r})|$ , and the photon-gluon mixed fields [13]:

$$\mathcal{A} \equiv \frac{\sqrt{3}g\mathbf{A} - 2e\mathbf{A}^8}{6g_{\text{CFL}}}, \quad \mathcal{A}^8 \equiv \frac{\sqrt{3}g\mathbf{A}^8 + 2e\mathbf{A}}{6g_{\text{CFL}}}, \quad (9)$$

where  $g_{\text{CFL}} = \sqrt{3g^2 + 4e^2}/6$ . Then, we can express the thermodynamic potential density difference as

$$\begin{aligned} \Delta\Omega &= \bar{\alpha}(|\phi|^2 + |\chi|^2) + \beta_1(|\phi|^2 + |\chi|^2)^2 + \beta_2(|\phi|^4 + |\chi|^4/2) \\ &\quad + 2K_T |(\nabla - 2ig_{\text{CFL}}\mathcal{A}^8)\phi|^2 + 2K_T |(\nabla + ig_{\text{CFL}}\mathcal{A}^8)\chi|^2 + \frac{1}{2}(|\mathbf{B}|^2 + |\mathbf{B}^8|^2 - |\mathbf{H}_{\text{ext}}|^2), \end{aligned} \quad (10)$$

where  $\mathbf{B} = \nabla \times \mathcal{A}$  and  $\mathbf{B}^8 = \nabla \times \mathcal{A}^8$ . By extremizing this free energy difference with respect to the pairing gaps and gauge fields, we obtain the gap equations,

$$-2K_T(\nabla - 2ig_{\text{CFL}}\mathcal{A}^8)^2\phi + \bar{\alpha}\phi + 2\beta_1(|\phi|^2 + |\chi|^2)\phi + 2\beta_2|\phi|^2\phi = 0, \quad (11)$$

$$-2K_T(\nabla + ig_{\text{CFL}}\mathcal{A}^8)^2\chi + \bar{\alpha}\chi + 2\beta_1(|\phi|^2 + |\chi|^2)\chi + \beta_2|\chi|^2\chi = 0, \quad (12)$$

and the classical Maxwell equations for the photon-gluon mixed fields,

$$\begin{aligned} \nabla \times (\nabla \times \mathcal{A}^8) &= \text{Re}\{4iK_Tg_{\text{CFL}}[-2\phi^*(\nabla - 2ig_{\text{CFL}}\mathcal{A}^8)\phi + \chi^*(\nabla + ig_{\text{CFL}}\mathcal{A}^8)\chi]\} \\ &\equiv \mathcal{J}^8, \end{aligned} \quad (13)$$

$$\nabla \times (\nabla \times \mathcal{A}) = 0. \quad (14)$$

From Eqs. (13) and (14) we find that in the CFL state ( $|\phi| = |\chi|/\sqrt{2} = |\kappa_A|$ ), the mixed field  $\mathcal{A}^8$  is Meissner screened within a London penetration depth,

$$\lambda_{\text{CFL}} = \frac{1}{2\sqrt{6}K_Tg_{\text{CFL}}|\kappa_A|}, \quad (15)$$

whereas the mixed field  $\mathcal{A}$  is freely propagating.

The thermodynamic critical field,  $H_c$ , associated with  $\mathbf{B} = \nabla \times \mathbf{A}$  is the field at which the Gibbs free energy density of the normal state,  $G_n = \Omega_n - \mathbf{H}_{\text{ext}} \cdot \mathbf{B}$ , drops to that of the superconducting state,  $G_s = \Omega_s - \mathbf{H}_{\text{ext}} \cdot \mathbf{B}$ . Since  $\mathbf{B}^8$  is screened out in the CFL phase in bulk, one can obtain the Gibbs free energy difference as [9]

$$\Delta G \equiv G_s - G_n = -\frac{\bar{\alpha}^2}{4\beta_{\text{CFL}}} + \frac{e^2}{18g_{\text{CFL}}^2}|\mathbf{H}_{\text{ext}}|^2. \quad (16)$$

Then,

$$H_c = \frac{3}{2e\xi_{\text{CFL}}\lambda_{\text{CFL}}}, \quad (17)$$

where

$$\xi_{\text{CFL}} = \left(\frac{2K_T}{|\bar{\alpha}|}\right)^{1/2}, \quad (18)$$

is the Ginzburg-Landau coherence length. As discussed in Ref. [9], extrapolation of the weak coupling expression for  $H_c$  to low densities and temperatures indicates that the critical field  $H_c$  is typically  $\sim 10^{19}$  G, several orders of magnitude larger than canonical neutron star surface fields  $\sim 10^{12}$  G.

We conclude this section by asking whether or not the CFL condensate allows magnetic vortices associated with the field  $\mathcal{A}^8$  to form, i.e., whether it is type II or type I. In a standard method for distinguishing between type I and type II superconductors, one calculates the energy per unit area,  $\sigma_s$ , needed to form a planar surface separating the normal and superconducting material. At the thermodynamic critical field, (17), applied parallel to the surface, the surface is in mechanical equilibrium. For a surface perpendicular to the  $z$  axis, the surface energy can be written as the integral over  $z$  of the difference between the total Gibbs free energy density and the value of  $|z| \rightarrow \infty$  [9]:

$$\sigma_s = \int_{-\infty}^{\infty} dz [\Delta\Omega(z)|_{H_{\text{ext}} \rightarrow H_c} - H_c(|\mathbf{B}(z)| - H_c)]. \quad (19)$$

Because of the presence of the color-flavor unlocked component near the surface, the system remains type II, i.e.,  $\sigma_s < 0$ , even when the Ginzburg-Landau parameter,  $\kappa_{\text{CFL}} \equiv \lambda_{\text{CFL}}/\xi_{\text{CFL}}$ , becomes less than  $1/\sqrt{2}$  by a small amount [10]. This is a contrast to the case of ordinary superconductors in which the Ginzburg-Landau parameter is  $1/\sqrt{2}$  when the interfacial energy vanishes [14]. Detailed calculations [10] show that for  $\beta_1 = \beta_2$  the system remains type II for values of  $\kappa_{\text{CFL}}$  down to  $\simeq 0.589$ . As we shall see in Sec. IV, however, the properties of intervortex interactions imply a significantly narrower type II region.

### III. MAGNETIC RESPONSE IN THE LONDON LIMIT

We now examine the response of the CFL condensate to external magnetic fields by deriving the supercurrent  $\mathcal{J}^8$  in the London limit in which a length scale of the spatial variation of the condensate is large compared with the coherence length  $\xi_{\text{GL}}$ , corresponding to the core size of a magnetic vortex. In this limit, one can ignore the variation of the magnitude of the pairing gaps,  $\phi$  and  $\chi$ , as compared with the variation of their phases [9]. We may thus derive  $\mathcal{J}^8$  by substituting the ansatz (8) with  $|\phi(\mathbf{r})| = |\chi(\mathbf{r})|/\sqrt{2} = |\kappa_A|$  into Eq. (13). The result reads

$$\mathcal{J}^8 = 4K_T g_{\text{CFL}} |\kappa_A|^2 (\sqrt{3} \nabla \varphi_8 - 6g_{\text{CFL}} \mathcal{A}^8). \quad (20)$$

We thus find that this supercurrent can be induced by the gradient of the color-flavor  $SU(3)$  phase,  $\varphi_8$ . This feature is essential to magnetic vortices, but was ignored in Ref. [9]. From expression (20) we can examine the response properties of the CFL condensate.

We first consider the response to weak uniform magnetic fields. As discussed in Ref. [9], the response is characterized by imperfect diamagnetism, i.e., partial Meissner screening. As long as  $g \gg e$ , most of the field freely propagates in the form of  $\mathcal{B}$ , whereas the rest is included in  $\mathcal{B}^8$  and hence screened on a length scale of  $\lambda_{\text{CFL}}$ .

For high fields, it is interesting to consider the possible presence of magnetic vortices. We find from Eq. (20) that vortices can appear in such a way as to satisfy the flux quantization condition,

$$\oint dl \cdot (\mathcal{A}^8 + \lambda_{\text{CFL}}^2 \mathcal{J}^8) = \frac{2\pi n}{g_{\text{CFL}}} \equiv \phi_8 n, \quad (21)$$

where the integration is performed around a closed loop surrounding the vortex line,  $\phi_8$  is the flux quantum, and  $n$  is the winding number of the vortex. Whether vortices actually occur in equilibrium depends on the value of  $\kappa_{\text{CFL}}$ , as will be discussed in Sec. IV.

In the London limit we can analyze the structure, far away from the core, of a singly quantized ( $n = 1$ ) vortex and then estimate the lower critical field,  $H_{c1}$ , above which a single vortex starts to appear. Let us take the vortex to be aligned along the  $z$  axis and set  $\varphi_8 = 2\sqrt{3}\varphi$ , where  $\varphi$  is the azimuthal angle around the line. Then, the field equation (13) reduces to the London equation,

$$\mathcal{B}^8 + \lambda_{\text{CFL}}^2 \nabla \times (\nabla \times \mathcal{B}^8) = \frac{1}{2\sqrt{3}g_{\text{CFL}}} \nabla \times \nabla \varphi_8 = \frac{2\pi}{g_{\text{CFL}}} \delta(x)\delta(y)\hat{z}. \quad (22)$$

Note that this equation leads to Eq. (21) with  $n = 1$ .

As in ordinary type II superconductors [14], one can solve the London equation (22) and obtain the supercurrent density flowing in the azimuthal direction around the line as

$$\mathcal{J}^8 = \begin{cases} \frac{\phi_8}{2\pi\lambda_{\text{CFL}}^2 r} \hat{\varphi}, & \text{for } \xi_{\text{CFL}} \ll r \ll \lambda_{\text{CFL}}, \\ \frac{\phi_8}{2\pi\lambda_{\text{CFL}}^2} \left(\frac{\pi\lambda_{\text{CFL}}}{2r}\right)^{1/2} \hat{\varphi} \left[ \frac{1}{\lambda_{\text{CFL}}} + \frac{1}{2r} + \mathcal{O}\left(\frac{\lambda_{\text{CFL}}}{r^2}\right) \right] e^{-r/\lambda_{\text{CFL}}}, & \text{for } r \gg \lambda_{\text{CFL}}. \end{cases} \quad (23)$$

The decrease of this supercurrent at a scale of  $\lambda_{\text{CFL}}$  suggests that the field  $\mathcal{B}^8$  associated with the vortex can penetrate only up to such a scale, beyond which  $\mathcal{A}^8 \simeq (1/g_{\text{CFL}}r)\hat{\varphi}$  and thus  $\mathcal{B}^8 \simeq 0$ . Combining Eqs. (21) and (23), one can calculate the vortex line energy per unit length, which is composed of the sum of the magnetic and flow energies, as

$$T_L = \frac{\phi_8^2}{4\pi\lambda_{\text{CFL}}^2} \ln \kappa_{\text{CFL}}. \quad (24)$$

At the lower critical field  $H_{c1}$ , the line energy is balanced by the energy gain due to the magnetic induction  $\mathcal{B}^8 = \mathcal{B}_z^8 \hat{z}$ . The energy gain per unit volume is  $E_{\text{mag}} = -\mathcal{B}_z^8 \mathcal{H}^8$ , where  $\mathcal{H}^8 = (e/3g_{\text{CFL}})H_{c1}$  is the critical field associated with the

massive photon-gluon mixed field [see Eq. (9)]. Integrating over the volume including the vortex, one can estimate a total energy gain per unit length as  $-\phi_8(e/3g_{\text{CFL}})H_{c1}$ . Then,

$$H_{c1} = \frac{3}{2e\lambda_{\text{CFL}}^2} \ln \kappa_{\text{CFL}}. \quad (25)$$

Note that the logarithmic factor in this expression contains uncertainties of order unity.

#### IV. STRUCTURE OF MAGNETIC VORTICES

As shown in the previous section, the analyses in the London limit are useful in clarifying the global properties of the magnetic response in the CFL phase. However, it is important to examine the vortex structure near the core, e.g., in evaluating the upper critical field  $H_{c2}$  where the vortices essentially fuse and the system becomes normal. In this section we thus go back to the Ginzburg-Landau equations and examine their solutions. Using these results, we revisit the problem of how to distinguish between type I and type II superconductors.

It is useful to start with the linearized gap equations with respect to  $\phi$  and  $\chi$ :

$$-2K_T(\nabla - 2ig_{\text{CFL}}\mathcal{A}^8)^2\phi + \bar{\alpha}\phi = 0, \quad (26)$$

$$-2K_T(\nabla + ig_{\text{CFL}}\mathcal{A}^8)^2\chi + \bar{\alpha}\chi = 0. \quad (27)$$

This is because equations (26) and (27) can describe the situation near  $H_{c2}$  in which the pairing gaps are suppressed in magnitude. The critical condition for the existence of nontrivial solutions to at least one of these equations is satisfied when  $g_{\text{CFL}}|\mathcal{B}^8| = |\bar{\alpha}|/2K_T$ . In this situation, a nontrivial  $\chi$  solution to Eq. (27) occurs, while  $\phi = 0$ . Using Eq. (9) we thus obtain

$$H_{c2} = \frac{3}{e\xi_{\text{CFL}}^2}. \quad (28)$$

Combining Eqs. (17) and (28), we find that  $H_{c2}/H_c = 2\kappa_{\text{CFL}}$ . When  $H_{c2} > H_c$ , i.e.,  $\kappa_{\text{CFL}} > 1/2$ , magnetic vortices are expected to occur. This condition in fact disagrees with the criterion for type II superconductors as derived in Ref. [10] from the sign of the normal-super interfacial energy  $\sigma_s$  (see Sec. II). Note that in ordinary superconductors [14], the condition  $H_{c2} = H_c$  agrees with the condition  $\sigma_s = 0$ . The difference between these two cases arises from the fact that in the CFL case, magnetic vortices are characterized by the color-flavor locked and unlocked condensates, while in the ordinary case, they are characterized by only a single complex scalar condensate.

This two-field nature of the CFL vortices can be seen by substituting  $\phi(r) = |\kappa_A|\exp(2in\varphi)u(r)$ ,  $\chi(r) = \sqrt{2}|\kappa_A|\exp(-in\varphi)v(r)$ , and  $\mathcal{A}^8(r) = \mathcal{A}_\varphi^8(r)\hat{\varphi}$  into the field equations (11), (12), and (13). Then we obtain

$$-2K_T\left(\frac{d^2}{dr^2} + \frac{1}{r}\frac{d}{dr}\right)u + 8K_T\left(\frac{n}{r} - g_{\text{CFL}}\mathcal{A}_\varphi^8\right)^2u + \bar{\alpha}u + 2\beta_1|\kappa_A|^2(u^2 + 2v^2)u + 2\beta_2|\kappa_A|^2u^3 = 0, \quad (29)$$

$$-2K_T\left(\frac{d^2}{dr^2} + \frac{1}{r}\frac{d}{dr}\right)v + 2K_T\left(\frac{n}{r} - g_{\text{CFL}}\mathcal{A}_\varphi^8\right)^2v + \bar{\alpha}v + 2\beta_1|\kappa_A|^2(u^2 + 2v^2)v + 2\beta_2|\kappa_A|^2v^3 = 0, \quad (30)$$

$$-\frac{d}{dr}\frac{1}{r}\frac{d}{dr}r\mathcal{A}_\varphi^8 = \frac{1}{3g_{\text{CFL}}\lambda_{\text{CFL}}^2}(2u^2 + v^2)\left(\frac{n}{r} - g_{\text{CFL}}\mathcal{A}_\varphi^8\right). \quad (31)$$

In the limit  $r \rightarrow 0$ , the normalized gaps  $u$  and  $v$  and the gauge field  $\mathcal{A}_\varphi^8$  are suppressed in magnitude. Consequently, the gap equations reduce to

$$-\left(\frac{d^2}{dr^2} + \frac{1}{r}\frac{d}{dr}\right)u + 4\left(\frac{n}{r}\right)^2u \rightarrow 0, \quad (32)$$

$$-\left(\frac{d^2}{dr^2} + \frac{1}{r}\frac{d}{dr}\right)v + \left(\frac{n}{r}\right)^2v \rightarrow 0. \quad (33)$$

From Eqs. (32) and (33), we find that

$$u \rightarrow C_1 r^{2n}, \quad v \rightarrow C_2 r^n, \quad (34)$$

where  $C_1$  and  $C_2$  are real constants that can be determined by connecting the solution near the center ( $r = 0$ ) with that outside the core. We can then calculate the asymptotic behavior of  $\mathcal{A}_\varphi^8$  from

$$-\frac{d}{dr} \frac{1}{r} \frac{d}{dr} r \mathcal{A}_\varphi^8 \rightarrow \frac{1}{3g_{\text{CFL}} \lambda_{\text{CFL}}^2} (2u^2 + v^2) \frac{n}{r}; \quad (35)$$

the result reads

$$\mathcal{A}_\varphi^8 \rightarrow \frac{1}{2} \mathcal{B}_0^8 r - \frac{C_2^2}{12g_{\text{CFL}} \lambda_{\text{CFL}}^2 (n+1)} r^{2n+1}, \quad (36)$$

where  $\mathcal{B}_0^8 = \mathcal{B}_z^8(r=0)$ . Consequently,

$$\mathcal{B}_z^8 \rightarrow \mathcal{B}_0^8 - \frac{C_2^2}{6g_{\text{CFL}} \lambda_{\text{CFL}}^2} r^{2n}. \quad (37)$$

We remark that as  $r \rightarrow 0$ ,  $v$  dominates over  $u$ . From Eq. (8) we thus find that the color-flavor locked and unlocked condensates coexist in the vortex core and behave as  $r^n$  near the center. This is similar to the case near  $H_{c2}$  in which  $\phi$  essentially vanishes.

We proceed to examine the vortex structure outside the core ( $r \gg \xi_{\text{CFL}}$ ) by taking into account small deviations from the asymptotic behaviors discussed in Sec. III:  $\delta u(r) = u(r) - 1$ ,  $\delta v(r) = v(r) - 1$ , and  $\delta \mathcal{A}_\varphi^8(r) = \mathcal{A}_\varphi^8(r) - n/g_{\text{CFL}} r$ . The field equations of linear order in these deviations read

$$-2K_T \left( \frac{d^2}{dr^2} + \frac{1}{r} \frac{d}{dr} \right) \delta u + [\bar{\alpha} + (10\beta_1 + 6\beta_2) |\kappa_A|^2] \delta u + 8\beta_1 |\kappa_A|^2 \delta v = 0, \quad (38)$$

$$-2K_T \left( \frac{d^2}{dr^2} + \frac{1}{r} \frac{d}{dr} \right) \delta v + [\bar{\alpha} + (14\beta_1 + 6\beta_2) |\kappa_A|^2] \delta v + 4\beta_1 |\kappa_A|^2 \delta u = 0, \quad (39)$$

$$\frac{d}{dr} \frac{1}{r} \frac{d}{dr} r \delta \mathcal{A}_\varphi^8 = \frac{1}{\lambda_{\text{CFL}}^2} \delta \mathcal{A}_\varphi^8. \quad (40)$$

It is convenient to diagonalize Eqs. (38) and (39) as

$$\left( \frac{d^2}{dr^2} + \frac{1}{r} \frac{d}{dr} \right) \frac{\delta u + 2\delta v}{3} = \frac{2}{\xi_{\text{CFL}}^2} \frac{\delta u + 2\delta v}{3}, \quad (41)$$

$$\left( \frac{d^2}{dr^2} + \frac{1}{r} \frac{d}{dr} \right) \frac{2(\delta u - \delta v)}{\sqrt{3}} = \frac{2}{\epsilon \xi_{\text{CFL}}^2} \frac{2(\delta u - \delta v)}{\sqrt{3}}, \quad (42)$$

where  $\epsilon = 3\bar{\beta}_{\text{CFL}}/\beta_2$ . Note that  $(\delta u + 2\delta v)/3$  represents a change in magnitude of the CFL condensate from the homogeneous one, whereas  $2(\delta u - \delta v)/\sqrt{3}$  represents the magnitude of the color-flavor unlocked condensate [see Eq. (8)]. We thus find from Eqs. (41) and (42) as well as the  $r \rightarrow 0$  behaviors discussed above that the magnitude of the CFL condensate increases with  $r$  in proportion to  $r^n$  near the vortex center and, above a scale of  $\xi_{\text{CFL}}/\sqrt{2}$ , approaches exponentially the homogeneous solution ( $u = v = 1$ ); the magnitude of the color-flavor unlocked condensate increases with  $r$  in proportion to  $r^n$  near the vortex center and, above a scale of  $\sqrt{\epsilon/2} \xi_{\text{CFL}}$ , decreases exponentially to zero. We remark that for  $r \gg \lambda_{\text{CFL}}$ ,  $\delta \mathcal{A}_\varphi^8$  follows the London limit behavior of the supercurrent (23) via  $\delta \mathcal{A}_\varphi^8 = -n\lambda_{\text{CFL}}^2 |\mathcal{J}^8|$ , leading to  $\mathcal{B}_z^8 \simeq (n\phi_8/2\pi\lambda_{\text{CFL}}^2)(\pi\lambda_{\text{CFL}}/2r)^{1/2} \exp(-r/\lambda_{\text{CFL}})$ . The vortex structure thus clarified is schematically illustrated in Fig. 1.

The parameter  $\epsilon = 3\bar{\beta}_{\text{CFL}}/\beta_2$  characterizing the scale of the spatial variation of the color-flavor unlocked condensate plays a important role in determining the nature of the interaction between widely separated vortices. For the purpose of estimating the intervortex interaction, it is instructive to write down the solutions to Eqs. (40), (41), and (42) as

$$\ln(g_{\text{CFL}} \lambda_{\text{CFL}} \delta \mathcal{A}_\varphi^8) \simeq \ln \left[ K_1 \left( \frac{r}{\lambda_{\text{CFL}}} \right) \right] + \mathcal{O}(1), \quad (43)$$

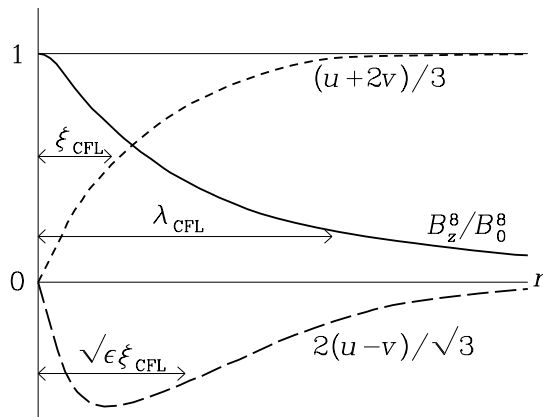


FIG. 1: Schematic variation of the mixed field  $B_z^8$  (solid line), the CFL condensate  $(u+2v)/3$  (dotted line), and the color-flavor unlocked condensate  $2(u-v)/\sqrt{3}$  (dashed line) for a singly quantized vortex ( $\lambda_{\text{CFL}} > \sqrt{\epsilon}\xi_{\text{CFL}} > \xi_{\text{CFL}}$ ).

$$\ln \frac{\delta u + 2\delta v}{3} \simeq \ln \left[ K_0 \left( \frac{\sqrt{2}r}{\xi_{\text{CFL}}} \right) \right] + \mathcal{O}(1), \quad (44)$$

$$\ln \frac{2(\delta u - \delta v)}{\sqrt{3}} \simeq \ln \left[ K_0 \left( \frac{\sqrt{2}r}{\sqrt{\epsilon}\xi_{\text{CFL}}} \right) \right] + \mathcal{O}(1), \quad (45)$$

where  $K_m$  are the  $m$ th modified Bessel functions. Then, following Ref. [15], one can estimate the interaction energy per unit length of two vortices at large separation  $a_v$  as

$$U(a_v) \simeq K_T |\kappa_A|^2 \left[ C_3 K_0 \left( \frac{a_v}{\lambda_{\text{CFL}}} \right) - C_4 K_0 \left( \frac{\sqrt{2}a_v}{\xi_{\text{CFL}}} \right) - C_5 K_0 \left( \frac{\sqrt{2}a_v}{\sqrt{\epsilon}\xi_{\text{CFL}}} \right) \right], \quad (46)$$

where  $C_3$ ,  $C_4$ , and  $C_5$  are positive dimensionless constants. Since  $K_0(x)$  is positive definite and decreases with  $x$ , the term associated with  $\lambda_{\text{CFL}}$  in Eq. (46) induces repulsion between the vortices, while the terms associated with  $\xi_{\text{CFL}}$  induce attraction. This reflects the fact that the total magnetic energy of the two vortices becomes larger for smaller intervortex separation, while the total loss of the condensation energy arising from the two vortices becomes smaller.

One of the conditions for type II (I) superconductors is that the intervortex interaction is repulsive (attractive) at large separation. In the case of repulsion, a vortex lattice is stable, while in the case of attraction, widely separated vortices tend to approach each other more and more closely. From Eq. (46), whose sign is dominated by the exponential behavior of the  $K_0$  functions [ $\ln K_0(x) = -x + \mathcal{O}(\ln x)$  for large  $x$ ], we find that the intervortex interaction is repulsive when  $\kappa_{\text{CFL}} > \max(1, \sqrt{\epsilon})/\sqrt{2}$ . We thus see the role played by  $\epsilon$  in determining the nature of the intervortex interaction. Note that  $\epsilon = 4$  in weak coupling.

The type II region is most strongly restricted by the condition that the intervortex interaction is repulsive. In this case, the critical value of  $\kappa_{\text{CFL}}$  is equal to or even larger than  $1/\sqrt{2}$ , while the value of  $\kappa_{\text{CFL}}$  at  $\sigma_s = 0$  and that at  $H_c = H_{c2}$  are smaller than  $1/\sqrt{2}$ . This is a contrast to the case of ordinary superconductors in which, owing to the simple order-parameter structure, all three critical values of the Ginzburg-Landau parameter are degenerate at  $1/\sqrt{2}$ . We remark that in weak coupling, where  $\kappa_{\text{CFL}} = \sqrt{6/7\zeta(3)}(6\pi^2 T_c/g_{\text{CFL}}\mu) \ll \sqrt{2}$  [10], the CFL condensate near  $T_c$  is deep within the type I region. However, it is still uncertain whether it is type I or type II at low densities where  $T_c$  can be  $\sim 0.1\mu$  and  $g_{\text{CFL}} \sim 1$  [9]. This uncertainty affects the estimates of  $H_{c1}$  and  $H_{c2}$  since  $H_{c2} = 2\kappa_{\text{CFL}}H_c$  and  $H_{c1} = (\kappa_{\text{CFL}}^{-1} \ln \kappa_{\text{CFL}})H_c$ .

## V. CONCLUSION

Within Ginzburg-Landau theory, we have derived the lower and upper critical fields,  $H_{c1}$  and  $H_{c2}$ , for the CFL state, as well as the critical Ginzburg-Landau parameter that distinguishes type I and type II superconductors. In doing so, we have examined the structure of a magnetic vortex near the center and outside the core. This vortex is associated with the winding of the  $SU(3)$  phase in color-flavor space, rather than the  $U(1)$  electromagnetic phase, and hence allows the presence of a color-flavor unlocked condensate in the core. We have found that the nature of the intervortex interaction, controlled by the color-flavor unlocked condensate, provides a stringent constraint on the type II regime.

Application of the present analyses to the magnetic structure and evolution of neutron stars is not straightforward. Not only does it require the extrapolation of the weak coupling results near  $T_c$  to low densities and temperatures, but also the clarification of a role of nonzero quark masses and neutrality of electric and color charge in modifying the CFL condensate at finite temperatures [16, 17, 18]. Due to uncertainties associated with the extrapolation, it is still open whether the CFL condensate, if occurring in stars, would be type I or type II. How nonzero quark masses and charge neutrality affect the response to magnetic fields is another open problem. Moreover, as discussed in Ref. [9], to assess the actual situations possible in neutron stars one must take into account the history of the expulsion of the magnetic field and the possibility of freezing in of the magnetic field.

## Acknowledgments

We thank Gordon Baym for critical reading of the original manuscript and Ioannis Giannakis and Hai-cang Ren for helpful comments. We are grateful to the Institute for Nuclear Theory at the University of Washington for its hospitality and to the Department of Energy for partial support during the completion of this work.

- 
- [1] See, e.g., K. Rajagopal and F. Wilczek, in *At the Frontier of Particle Physics, Handbook of QCD, Boris Ioffe Festschrift, V. 3*, edited by M. Shifman (World Scientific, Singapore, 2001), p. 2061; M.G. Alford, *Annu. Rev. Nucl. Part. Sci.* **51**, 131 (2001).
  - [2] M. Alford, K. Rajagopal, and F. Wilczek, *Nucl. Phys.* **B537**, 443 (1999).
  - [3] D. Bailin and A. Love, *Phys. Rep.* **107**, 325 (1984).
  - [4] D.K. Hong and S.D.H. Hsu, *Phys. Rev. D* **68**, 034011 (2003).
  - [5] K. Iida and G. Baym, *Phys. Rev. D* **63**, 074018 (2001); *Phys. Rev. D* **66**, 059903(E) (2002).
  - [6] See, e.g., M. Huang, hep-ph/0409167.
  - [7] D. Blaschke and D. Sedrakian, nucl-th/0006038.
  - [8] M. Alford, J. Berges, and K. Rajagopal, *Nucl. Phys.* **B571**, 269 (2000).
  - [9] K. Iida and G. Baym, *Phys. Rev. D* **66**, 014015 (2002).
  - [10] I. Giannakis and H.-C. Ren, *Nucl. Phys.* **B669**, 462 (2003).
  - [11] Note the difference from the convention in Ref. [9] in which  $\lambda^8 = \text{diag}(1, 1, -2)/\sqrt{3}$ . The present convention is useful since the corresponding color part in the covariant derivative is proportional to the electromagnetic part.
  - [12] I. Giannakis and H.-C. Ren, *Phys. Rev. D* **65**, 054017 (2002).
  - [13] E.V. Gorbar, *Phys. Rev. D* **62**, 014007 (2000).
  - [14] P.G. de Gennes, *Superconductivity of Metals and Alloys* (Benjamin, New York, 1966).
  - [15] R. MacKenzie, M.-A. Vachon, and U.F. Wichoski, *Phys. Rev. D* **67**, 105024 (2003).
  - [16] K. Iida, T. Matsuura, M. Tachibana, and T. Hatsuda, *Phys. Rev. Lett.* **93**, 132001 (2004); hep-ph/0411356.
  - [17] S.B. Rüster, I.A. Shovkovy, and D.H. Rischke, *Nucl. Phys.* **A743**, 127 (2004).
  - [18] K. Fukushima, C. Kouvaris, and K. Rajagopal, hep-ph/0408322.